Energy Correlation in Wirelessly Powered Networks

Na Deng*† and Martin Haenggi‡
*School of Information & Communication Engineering, Dalian University of Technology, Dalian, 116024, China
†National Mobile Communications Research Laboratory, Southeast University, Nanjing, 210096, China
‡Dept. of Electrical Engineering, University of Notre Dame, Notre Dame, IN, 46556, USA
Email:*†dengna@dlut.edu.cn, ‡mhaenggi@nd.edu

***Abstract*—This paper investigates the spatial correlation of the energy harvested from a Poisson field of RF power sources. Specifically, we focus on two energy harvesting models—one dependent on distance alone and the other with more practical factors taken into account—with the aim of showing how the actual point process of nodes that successfully harvest energy looks visually and characterize the pair correlation functions for such point process under the two models theoretically. It turns out that for both models the resulting process of the energized nodes exhibits positive correlations. Therefore, we further approximate the point process formed by active RF-powered nodes with a fitted Poisson cluster process, which is shown to provide a good approximation of the success probability in the information transmission. An important conclusion is that though the Poisson point process has been widely used to model the spatial configuration of energized nodes, it is inadequate for modeling the locations of the active RF-powered nodes due to the positive correlation.**

I. Introduction

As a new enabler for energy harvesting, wireless energy transfer (WET) is anticipated to have great applications in future energy constrained wireless communication networks [1]. This integration of RF-based energy harvesting in communication networks renders the spatial structure of transmitters (including the RF sources and the RF-powered nodes) even more crucial since it not only determines the mutual interference and the signal-interference-plus-noise ratio (SINR) performance in conventional communications but also the energy that can be harvested in WET. As a consequence, stochastic geometry models for wirelessly powered networks have recently received widespread attention due to their capability of capturing the irregularity and variability of the node configurations in real networks and providing theoretical insights [2–5].

The Poisson point process (PPP) has been by far the most popular spatial model for various types of wireless networks. This is because the PPP model has several convenient features, such as the independence between points in disjoint regions and the simple form of the probability generating functional (PGFL) [6]. Therefore, the PPP model of RF transmitters provides a tractable analysis for the energy outage probability [2] as well as its meta distribution in the energy harvesting phase [7]. As for the information transmission phase, the analysis in previous works is mostly based on the assumption that the active RF-powered nodes, which are the nodes that successfully harvest energy from a Poisson field of RF transmitters, are formed by independently thinning the Poisson distributed RF-powered nodes [3, 5, 7]. That is to say, the active RF-powered nodes are assumed to form a PPP again. However, this does not seem realistic since if a node succeeds in harvesting energy, a nearby node will have a good chance of succeeding also, and vice versa. In other words, the nodes that successfully harvest energy from a Poisson field of transmitters are not mutually independent but *spatially correlated*. Therefore, it is important to fully characterize the spatial correlation of the energy harvested from RF transmitters and the corresponding effect on the performance of communication systems, which, to our best knowledge, has not been studied previously.

In this paper, we investigate the impact of energy correlation in wirelessly powered networks, i.e., the spatial correlation of nodes that successfully harvest enough energy from a Poisson field of RF transmitters, or equivalently, how likely a node at a particular location succeeds in harvesting energy when a nearby node succeeds. We start with a simple model dependent on distance alone, where a RF-powered node is active if and only if there is at least one RF transmitter within a certain distance, and then extend it to a practical case that includes more factors. Under the two models, the active RF-powered nodes in the information transmission phase form a new point process, named the *energized point process* (EPP). To characterize the spatial correlation of the EPP, we derive the first- and second-order (pair correlation function) statistics for these two energy harvesting models. It is clearly shown that the EPPs under both models exhibit positive correlations, which means "attraction" exists between the locations of active RF-powered nodes. To show the effect of such spatial correlation on the communication performance, we further use a fitted Poisson cluster process (PCP) to approximate the EPP, which turns out to provide a good approximation of the transmission success probability.

II. System model

We consider a wireless network powered solely by ambient RF transmitters (which may include cellular base stations, digital TV towers, WiFi hotspots, etc.), where the locations of RF transmitters and RF-powered nodes follow two point processes Φ_{p} and Φ_{d}, respectively. We first formally define the EPP, which is formed by the RF-powered nodes that succeed in harvesting enough energy for subsequent transmission.

A. The Energized Point Process

Definition 1 (Energized point process, EPP). *Let Φ_{p} and Φ_{d} be two point processes. The energized point process Φ_{e} is defined as*

$$\Phi_{\mathrm{e}} \triangleq \{x \in \Phi_{\mathrm{d}} \colon E(x, \Phi_{\mathrm{p}}) = 1\}, \tag{1}$$

where E is the energy indicator function describing whether enough energy can be harvested from Φ_{p} at location x.

In this paper, the two point processes Φ_{p} and Φ_{d} are assumed to be two independent homogeneous PPPs of densities λ_{p} and λ_{d}, respectively. The resulting EPP is a dependent thinning of Φ_{d} and can be viewed as a Cox process [6, Def. 3.3] with intensity field $\kappa(x) = \lambda_{\mathrm{d}} \mathbf{1}(E(x, \Phi_{\mathrm{p}}) = 1)$, where $\mathbf{1}(\cdot)$ denotes the indicator function.

B. Simplified Energy Harvesting Model (SEHM)

Since the harvested energy depends on the locations of the nearby RF transmitters, we first consider a simplified model where a RF-powered node succeeds in harvesting enough energy if and only if there is at least one RF transmitter within distance R. This can be formulated as

$$E(x, \Phi_{\mathrm{p}}) = \mathbf{1}(\Phi_{\mathrm{p}}(b(x, R)) > 0), \tag{2}$$

where $b(x, r)$ is the disk centered at x of radius r and $\Phi(B)$ is the number of points of the point process Φ falling in B.

C. Practical Energy Harvesting Model (PEHM)

Furthermore, we consider a practical energy harvesting model that includes more factors, such as channel gains, random effects in the energy detection and conversion at the receiver side, etc. The channel (power) gain between transmitter x and receiver y is given by $h_{xy}\ell(x - y)$ where h_{xy} models the small-scale fading and $\ell(x - y)$ represents the large-scale path loss. We assume that all fading coefficients are i.i.d. exponential (Rayleigh fading) with $\mathbb{E}(h_{xy}) = 1$, and $\ell(x) = \|x\|^{-\alpha}$, where α is the path loss exponent. The transmit power of RF transmitters is assumed to be one. Using the energy harvesting model in [8], the harvested energy $\varepsilon(x, \Phi_{\mathrm{p}})$ at the RF-powered node x can be quantified as

$$\varepsilon(x, \Phi_{\mathrm{p}}) = \frac{\nu\eta\rho}{1 + F} \sum_{y \in \Phi_{\mathrm{p}}} h_{yx}\ell(y - x), \tag{3}$$

where the term $\frac{\nu}{1+F}$ captures the randomness in the detection of the actual harvested energy, F follows an exponential distribution with parameter ζ, and ν is chosen so that $\frac{\nu}{1+F}$ has an expectation of 1, i.e., $\nu = \frac{1}{-\zeta e^{\zeta}\,\mathrm{Ei}(-\zeta)}$, where Ei is the exponential integral function defined by $\mathrm{Ei}(x) = -\int_{-x}^{\infty} e^{-t}/t\mathrm{d}t$. ρ is the efficiency of the conversion from RF to DC power and η is the fraction in a time slot for energy harvesting process. Therefore, in this model, we have

$$E(x, \Phi_{\mathrm{p}}) = \mathbf{1}(\varepsilon(x, \Phi_{\mathrm{p}}) > \xi), \tag{4}$$

where ξ is the energy threshold.

Fig. 1 shows a comparison between the realizations of the PEHM-based EPP and PPP with the same density. It is observed that the spatial distribution of the active RF-powered nodes exhibits clustering relative to the PPP.

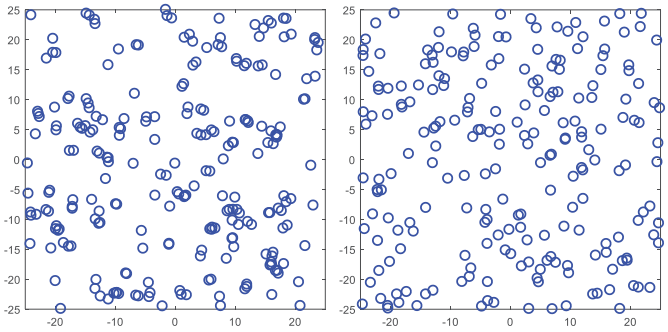

Fig. 1. Comparison of the EPP (left) and PPP (right). For the EPP, the PEHM is adopted with default parameter setting. For both point processes, the density is 0.0922.

TABLE I. Symbols and descriptions

Symbol	Description	Default
λ_{p}	The density of RF transmitters PPP	0.1
λ_{d}	The density of RF-powered nodes PPP	1
α	The path loss exponent	4
η	The fraction of time for energy harvesting	0.5
R	The distance threshold in the simplified model	1
ρ	The efficiency of energy harvesting	0.3 [8]
ζ	The parameter in the energy harvesting model	0.01 [8]

D. Communication Model

We consider that RF-powered nodes adopt a time-switched "harvest-then-transmit" strategy in each time slot, and RF transmitters use frequencies outside the data band and hence cause no interference to the information transmission of RF-powered nodes. Specifically, in each time slot, each RF-powered node first uses a fraction η of the time slot to harvest energy from RF transmitters and then transmit the information to its corresponding receiver during the remaining $1 - \eta$ fraction of time if the harvested energy satisfies the minimum requirement for signal transmission. Each RF-powered node is assumed to merely utilize the instantaneously harvested RF energy from RF transmitters to supply its operation and to have a dedicated receiver at distance r_{d} in a random orientation, i.e., the RF-powered nodes and their receivers form a Poisson bipolar network [6, Def. 5.8]. Hence, the active RF-powered nodes and their receivers form a Cox bipolar network. The transmit power of RF-powered nodes is assumed to be one.

Table I summarizes the notations of the parameters in the network model with their descriptions, and default values are given where applicable.

III. Analytical Results for the EPP

In this section, we provide analytical results for the first- and second-order statistics to characterize the properties of the EPP. Since a translated and rotated version of Φ_{e} can be obtained by translating and rotating Φ_{p} and Φ_{d}, which are motion-invariant, Φ_{e} is motion-invariant. As a result, the first-order statistic, i.e., the density, denoted as λ_{e}, is obtained by deriving the success probability p_{s} of the energy harvesting of

the RF-powered node at the origin, i.e., $p_{\rm s}=\mathbb{P}(E(o,\Phi_{\rm p})=1)$ and $\lambda_{\rm e}=p_{\rm s}\lambda_{\rm d}$. For the second-order statistic, the pair correlation function (pcf) $g(x,y)$ [6, Def. 6.6] is usually used to describe the degree of correlation between two distinct points in the point process, and for a motion-invariant process, the pcf depends only on the distance $r=\|x-y\|$, i.e., $g(x,y)=g(r)$. The following theorem gives a general expression of the pcf for the EPP.

Theorem 1. *The pair correlation function of the EPP $\Phi_{\rm e}$ is*

$$g_{\rm e}(r)=\frac{p_{\rm joint}(r)}{p_{\rm s}^2}, \tag{5}$$

where $p_{\rm joint}(r)=\mathbb{P}(E(o,\Phi_{\rm p})=1,E(z_r,\Phi_{\rm p})=1)$ is the joint success probability that both the two points at locations $z_r=(r,0)$ and o succeed in energy harvesting and thus are retained in $\Phi_{\rm e}$.

Proof: According to [6, Lemma 6.9], the pcf is given by

$$g(r)=\frac{1}{2\pi r}\frac{\rm d}{{\rm d}r}K(r), \tag{6}$$

where $K(r)$ is Ripley's K function [6, Def. 6.8], defined as

$$K(r)=\frac{1}{\lambda}\mathbb{E}_o^!\Phi\big(b(o,r)\big), \tag{7}$$

where $\mathbb{E}_o^!$ denotes the expectation with respect to the reduced Palm distribution of Φ given that $o\in\Phi$. We first calculate $\mathbb{E}_o^!\Phi_{\rm e}\big(b(o,r)\big)$, i.e., the mean number of extra points within distance r of the origin. A point of $\Phi_{\rm d}$ at location x with distance $u=\|x\|$ is retained in $\Phi_{\rm e}$ if $E(x,\Phi_{\rm p})=1$ under the condition that $E(o,\Phi_{\rm p})=1$ (because the point at the origin is already retained in $\Phi_{\rm e}$). And the motion-invariance of $\Phi_{\rm d}$ makes the condition of $E(x,\Phi_{\rm p})=1$ equivalent to that with $x=(u,0)$. Since the density of the points in $\Phi_{\rm d}$ at distance u is $2\pi\lambda_{\rm d}u$, we have

$$\begin{aligned}&\mathbb{E}_o^!\Phi_{\rm e}\big(b(o,r)\big)\\&=2\pi\lambda_{\rm d}\int_0^r\mathbb{P}(E((u,0),\Phi_{\rm p})=1\mid E(o,\Phi_{\rm p})=1)u{\rm d}u\\&=\frac{2\pi\lambda_{\rm d}}{p_{\rm s}}\int_0^r\mathbb{P}(E((u,0),\Phi_{\rm p})=1,E(o,\Phi_{\rm p})=1)u{\rm d}u.\end{aligned} \tag{8}$$

The final result is obtained by substituting (8) and (7) into (6). ∎

A. The SEHM-based EPP

From the simplified model, it is easy to derive the probability that a point of $\Phi_{\rm d}$ succeeds in harvesting energy and is retained, given by

$$p_{\rm s}=1-\exp(-\lambda_{\rm p}\pi R^2), \tag{9}$$

and the density of the EPP is $\lambda_{\rm e}=\lambda_{\rm d}(1-e^{-\lambda_{\rm p}\pi R^2})$.

Letting $V_r(R)=b(o,R)\cap b(z_r,R)$, the event that both the two points z_r and o succeed in energy harvesting is partitioned into two disjoint events: one is that at least one RF transmitter falls in $V_r(R)$; the other is that at least one RF transmitter falls in $b(o,R)\setminus V_r(R)$ and $b(z_r,R)\setminus V_r(R)$, respectively, conditioning on that no RF transmitter falls in $V_r(R)$. According to the total probability law, we have

$$\begin{aligned}p_{\rm joint}(r)&=1-e^{-\lambda_{\rm p}A_R(r)}+e^{-\lambda_{\rm p}A_R(r)}\\&\quad\times\Big(1-e^{-\lambda_{\rm p}(\pi R^2-A_R(r))}\Big)^2\\&=1-2e^{-\lambda_{\rm p}\pi R^2}+e^{-\lambda_{\rm p}\left(2\pi R^2-A_R(r)\right)},\end{aligned} \tag{10}$$

where

$$A_R(r)=2R^2\arccos\left(\frac{r}{2R}\right)-r\sqrt{R^2-\frac{r^2}{4}} \tag{11}$$

is the intersection area of two disks of radius R at distance r. Hence the pcf of the SEHM-based EPP is

$$g_{\rm e}(r)=1+\frac{e^{-2\lambda_{\rm p}\pi R^2}\left(e^{\lambda_{\rm p}A_R(r)}-1\right)}{(1-e^{-\lambda_{\rm p}\pi R^2})^2}. \tag{12}$$

Since $g_{\rm e}(r)>1$, the EPP exhibits clustering.

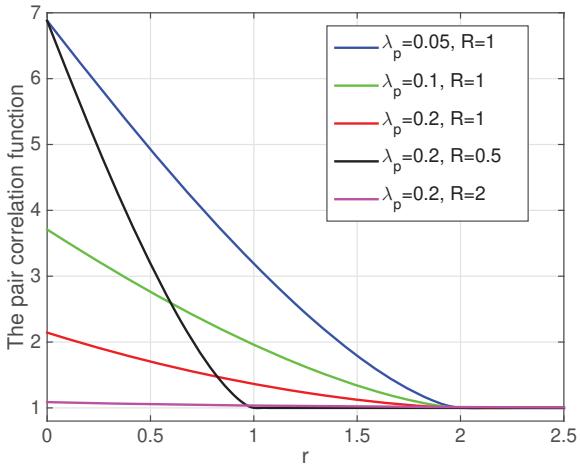

Fig. 2. The pcfs of the SEHM-based EPP with different $\lambda_{\rm p}$ and R.

Fig. 2 shows how the density of the RF transmitters and the threshold R affect the correlation between two points in the EPP. It is observed that a smaller $\lambda_{\rm p}$ or R leads to stronger clustering, which means the clustering behavior is increasingly prominent as the ambient RF transmitters become sparse or the energy correlation region becomes small (or, equivalently, fewer RF-powered nodes can be retained).

B. The PEHM-based EPP

Under this model, we first give an asymptotical upper bound on the density of the EPP, which is then proven to be very accurate with well controlled and mathematically quantified gaps.

Theorem 2. *Let $\delta\triangleq 2/\alpha$, $\bar{\xi}\triangleq\zeta\nu\eta\rho/\xi$ and*

$$\hat{p}_{\rm s}(\xi)\triangleq 1-\exp\Big(-\pi\lambda_{\rm p}\frac{\pi\delta}{\sin(\pi\delta)}\bar{\xi}^{\delta}\Big). \tag{13}$$

The success probability of the energy harvesting for PEHM is asymptotically upper bounded as $p_{\rm s}\lesssim\hat{p}_{\rm s}(\xi)$, and the density

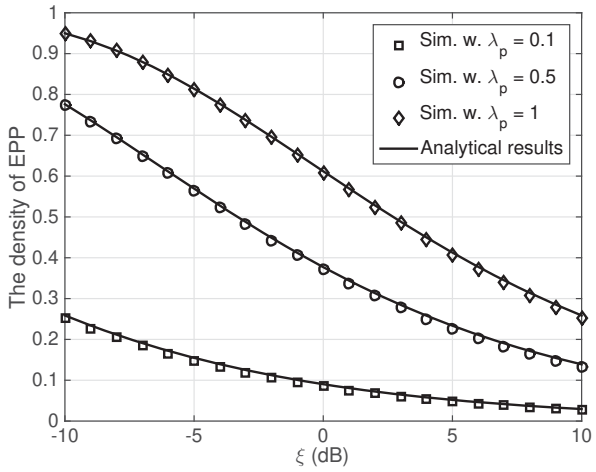

Fig. 3. The density of the PEHM-based EPP versus ξ for different $\lambda_{\rm p}$.

of the EPP follows $\lambda_{\rm e} \lesssim \lambda_{\rm d} p_{\rm s}(\xi)$*, where '*$\lesssim$*' stands for an asymptotic upper bound, i.e.,* $\exists t > 0$ *s.t.* $p_{\rm s} < \hat{p}_{\rm s}(\xi)\ \forall \zeta < t$.

Proof: Letting $I_o = \sum_{y \in \Phi_{\rm p}} h_{yo}\ell(y)$, the success probability of the energy harvesting is given by

$$\begin{aligned} p_{\rm s} &= \mathbb{P}\Big(\frac{\nu\eta\rho}{F+1} I_o \geq \xi\Big) \\ &\leq \mathbb{P}\Big(F \leq \frac{\nu\eta\rho}{\xi} I_o\Big) \\ &= 1 - \mathbb{E}\Big[\exp\Big(-\bar{\xi} I_o\Big)\Big] \\ &\overset{(a)}{=} 1 - \exp\Big(-\pi\lambda_{\rm p}\frac{\pi\delta}{\sin(\pi\delta)}\bar{\xi}^{\delta}\Big), \end{aligned} \tag{14}$$

where step (a) uses the Laplace transform of the interference in Poisson networks [6, Sec. 5.17]. Hence, the density $\lambda_{\rm e}$ of the EPP $\Phi_{\rm e}$ is given by

$$\lambda_{\rm e} = \lambda_{\rm p} p_{\rm s} \leq \lambda_{\rm p}\hat{p}_{\rm s}(\xi). \tag{15}$$

Next, we explain the accuracy of the above bound. Letting $Y = \nu\eta\rho I_o/\xi$, we have

$$\begin{aligned} &p_{\rm s} - \hat{p}_{\rm s}(\xi) \\ &= \mathbb{P}(F \leq Y - 1) - \mathbb{P}(F \leq Y) \\ &= \mathbb{P}(F > Y) - \mathbb{P}(F > Y - 1) \\ &= \mathbb{E}_Y\Big[\big(e^{-\zeta Y} - e^{-\zeta(Y-1)}\big)\mathbf{1}_{Y\geq 1} + \big(e^{-\zeta Y} - 1\big)\mathbf{1}_{Y<1}\Big] \\ &\geq \mathbb{E}_Y\Big[\big(e^{-\zeta} - 1\big)\mathbf{1}_{Y\geq 1} + \big(e^{-\zeta} - 1\big)\mathbf{1}_{Y<1}\Big] \\ &= e^{-\zeta} - 1. \end{aligned} \tag{16}$$

Since $p_{\rm s} \leq \hat{p}_{\rm s}(\xi)$, $p_{\rm s}$ is bounded by

$$\hat{p}_{\rm s}(\xi) + e^{-\zeta} - 1 \leq p_{\rm s} \leq \hat{p}_{\rm s}(\xi). \tag{17}$$

Thus $p_{\rm s} \to \hat{p}_{\rm s}(\xi)$ as $\zeta \to 0$, and $p_{\rm s} \lesssim \hat{p}_{\rm s}(\xi)$. ■

Fig. 3 shows the density of the EPP with the comparison between the analytical and simulation results. The analytical bounding result for the density is shown to provide an accurate approximation to the simulation result. In addition, the density of the EPP becomes smaller as the increase of ξ or the decrease of $\lambda_{\rm p}$, which implies that either the dense deployment of RF transmitters or the low energy consumption of wireless powered nodes allows more RF-powered nodes to be active in the information transmission phase.

The following theorem provides analytical results for bounding the joint success probability and approximating the pcf of the EPP. For notational convenience, we define $\psi(t, r, \theta) \triangleq \sqrt{t^2 + r^2 - 2rt\cos(\theta)}$.

Theorem 3. *Let*

$$\begin{aligned} \hat{p}_{\rm joint}(r) \triangleq\ & 1 - 2\exp\Big(-\pi\lambda_{\rm p}\frac{\pi\delta}{\sin(\pi\delta)}\bar{\xi}^{\delta}\Big) \\ &+ \exp\Big(-\lambda_{\rm p}\int_0^{\infty}\int_0^{2\pi}\chi(t,\theta)t\,{\rm d}t\,{\rm d}\theta\Big), \end{aligned} \tag{18}$$

where

$$\chi(t,\theta) = 1 - \frac{1}{(1+\bar{\xi}t^{-\alpha})(1+\bar{\xi})\psi(t,r,\theta)^{-\alpha}}. \tag{19}$$

The joint success probability of two points within distance r *for PEHM is asymptotically upper bounded as* $p_{\rm joint}(r) \lesssim \hat{p}_{\rm joint}(r)$ *and the corresponding pcf follows* $g_{\rm e}(r) \approx \hat{p}_{\rm joint}(r)/\hat{p}_{\rm s}^2$.

Proof: Letting $I_{z_r} = \sum_{y\in\Phi_{\rm p}} h_{yz_r}\ell(y - z_r)$, we have

$$\begin{aligned} p_{\rm joint}(r) &= \mathbb{P}(\varepsilon(z_r) > \xi, \varepsilon(o) > \xi) \\ &\leq \mathbb{P}\Big(F_o \leq \frac{\nu\eta\rho}{\xi} I_o, F_{z_r} \leq \frac{\nu\eta\rho}{\xi} I_{z_r}\Big) \\ &= \mathbb{E}\big[\big(1 - e^{-\bar{\xi}I_o}\big)\big(1 - e^{-\bar{\xi}I_{z_r}}\big)\big] \\ &= 1 - 2e^{-\pi\lambda_{\rm p}\frac{\pi\delta}{\sin(\pi\delta)}\bar{\xi}^{\delta}} + \mathbb{E}\big[e^{-\bar{\xi}(I_o + I_{z_r})}\big], \end{aligned} \tag{20}$$

where the PGFL of the PPP yields

$$\begin{aligned} \mathbb{E}\big[e^{-\bar{\xi}(I_o+I_{z_r})}\big] &= \mathbb{E}\Big[\prod_{x\in\Phi_{\rm p}}\frac{1}{\big(1+\bar{\xi}\ell(x)\big)\big(1+\bar{\xi}\ell(x-z_r)\big)}\Big] \\ &= \exp\Big(-\lambda_{\rm p}\int_0^{\infty}\int_0^{2\pi}\chi(t,\theta)t\,{\rm d}t\,{\rm d}\theta\Big). \end{aligned} \tag{21}$$

The asymptotic upper bound can be proved with a similar approach as in the proof of Thm. 2, and the pcf of the EPP is approximated through Thm. 1. ■

Fig. 4 illustrates the pcfs of the PEHM-based EPP, where the simulations are estimated through the inline function **pcf** in the **R language**. It shows that the analytical results in Thm. 3 provide a tight approximation; the small gap between the analytical and simulated curves vanishes as r increases, and also with increasing $\lambda_{\rm p}$. The slightly larger gap for small $\lambda_{\rm p}$ is a consequence of the fact that for small densities, it quickly becomes unlikely that a point has a neighbor within distance r, which makes it harder to accurately estimate the pcf. Also, the **pcf** function in **R** is implemented according

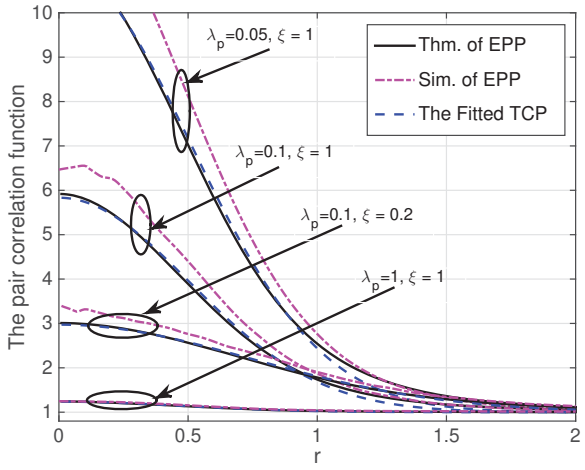

Fig. 4. The pcfs of the PEHM-based EPP with different $\lambda_{\rm p}$ and ξ.

to the definition in (6), which includes a division by r and a derivative w.r.t. r, and these operations are not numerically robust at small r. Furthermore, we observe that all the pcfs are larger than in the PPP case and decrease with the increase of r, which again demonstrates the clustering behavior of the active RF-powered nodes and the correlation becomes weaker with increasing inter-distance. Moreover, a smaller $\lambda_{\rm p}$ or a larger ξ leads to a larger pcf for a fixed r, which means that the correlation between two active RF-powered nodes is stronger with a smaller $\lambda_{\rm p}$ or a larger ξ. This is because whether a RF-powered node succeeds in harvesting enough energy is chiefly determined by its nearby (especially the nearest) RF transmitters, and it is more likely for different RF-powered nodes to have the same nearby (nearest) RF transmitters in a sparse deployment of RF transmitters.

IV. Success Probability of Information Transmission

For the information transmission phase, the properties of the desired signal and interference highly depend on the spatial distribution of the active RF-powered nodes, which determines the transmission success probability. Since the EPP is also a stationary point process, we condition on that the typical RF-powered node is located at the origin, i.e. $o \in \Phi_{\rm e}$, and the corresponding typical receiver is at $z = (r_{\rm d}, 0)$. Letting $\Phi_{\rm e}^! = \Phi_{\rm e} \setminus \{o\}$ and $I(z) = \sum_{x\in\Phi_{\rm e}^!} \ell(x-z)h_{xz}$ be the interference at the typical receiver, the received signal-to-interference ratio (SIR) of the typical receiver is given by

$$\mathrm{SIR} = \frac{r_{\rm d}^{-\alpha} h_{oz}}{\sum\limits_{x\in\Phi_{\rm e}^!} \ell(x-z)h_{xz}}, \tag{22}$$

and the success probability is defined as $P(\theta) \triangleq \mathbb{P}(\mathrm{SIR} > \theta)$ where θ is the SIR threshold. With signals subject to Rayleigh fading, the transmission success probability is the Laplace transform of $I(z)$ evaluated at $s = \theta r_{\rm d}^{\alpha}$, given by

$$P(\theta) = \mathcal{L}_{I(z)}(\theta r_{\rm d}^{\alpha}), \tag{23}$$

and the Laplace transform of $I(z)$ is

$$\begin{aligned}\mathcal{L}_{I(z)}(s) &= \mathbb{E}\exp\Big(-s\sum_{x\in\Phi_{\rm e}^!}\ell(x-z)h_{xz}\Big)\\ &= \mathbb{E}_{\Phi_{\rm e}^!}\Big(\prod_{x\in\Phi_{\rm e}^!}\frac{1}{1+s\ell(x-z)}\Big)\\ &= \mathbb{E}_o^!\Big(\prod_{x\in\Phi_{\rm e}}\frac{1}{1+s\ell(x-z)}\Big),\end{aligned} \tag{24}$$

where $\mathbb{E}_o^!$ denotes the expectation with respect to the reduced Palm distribution of the EPP, given that there is an active RF-powered node at the origin.

Due to the dependent thinning, an exact calculation of the success probability under the EPP model seems unfeasible. Thus next, we resort to approximating it with two common point processes, i.e., the PPP and PCP, which have explicit PGFL expressions. The benefits of such approximations is to provide an accurate yet tractable analysis of the performance in the information transmission phase in wirelessly powered networks, which can hardly be obtained by the EPP directly.

1) PPP Approximation: As a baseline model, we first approximate the EPP with a PPP using the first-order statistic $\lambda_{\rm s}$. From Slivnyak's theorem [6], conditioning on a point at the origin does not change the distribution of the rest of the process, and the reduced palm distribution is the same as the original PPP. Hence, $\mathcal{L}_{I(z)}(s)$ is approximated by

$$\mathcal{L}_{I_{\rm PPP}}(s) = \exp\Big(-\lambda_{\rm e}\pi\frac{\pi\delta}{\sin(\pi\delta)}s^{\delta}\Big), \tag{25}$$

and the success probability is approximated as

$$P(\theta) \approx \exp\Big(-\lambda_{\rm e}\frac{\pi^2\delta}{\sin(\pi\delta)}r_{\rm d}^2\theta^{\delta}\Big). \tag{26}$$

2) PCP Approximation: From the above discussion, the points in EPP are clustered. Since PCP also exhibits clustering and more importantly it leads to tractable results. Thus we provide another approximation of the EPP with a fitted PCP (e.g. the Thomas cluster process (TCP)) through matching the first- and second-order statistics.

First-order statistic matching yields

$$\lambda_{\rm e} = \lambda_l \bar{c}, \tag{27}$$

where λ_l is the density of parent points of the cluster process and $\bar{c}$ is the average number of points in a cluster. For the TCP with variance σ^2, the pcf is [6, Section 6.4]

$$g_{\rm T}(r) = 1 + \frac{1}{4\pi\lambda_l\sigma^2}\exp\left(-\frac{r^2}{4\sigma^2}\right), \tag{28}$$

where λ_l and σ are obtained using curve-fitting and $\bar{c}$ is then determined using (27). By using the **fmincon** function (minimizing the constrained nonlinear multivariable function) in **Matlab**, we fit the pcf of the TCP to the approximative analytical pcf of the EPP for different ζ and $\lambda_{\rm p}$. The fitting parameters of the TCP are listed in Table II, and Fig. 4 also illustrates the fitted pcf curves of the TCP. The results show that the EPP can be closely approximated by the TCP.

TABLE II. The fitting results for different $\lambda_{\rm p}$ and ζ

$\lambda_{\rm p}$	0.05	0.1	0.1	1
ξ	1	0.2	1	1
$\lambda_{\rm l}$	0.0616	0.1437	0.1288	3.0022
σ^2	0.1288	0.2807	0.1279	0.1116
$\bar{c}$	0.7498	1.3270	0.7011	0.2038

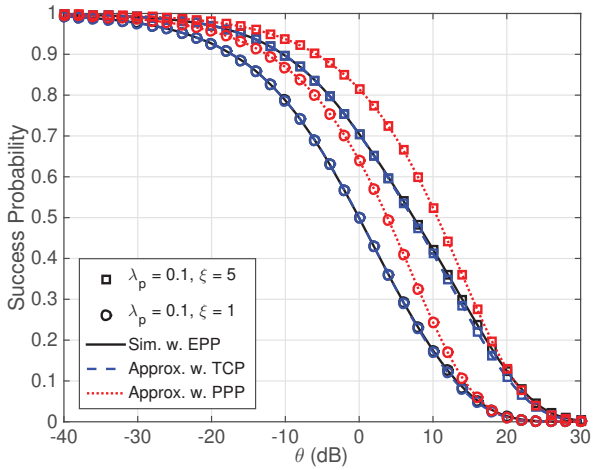

Fig. 5. The success probability with PPP and PCP approximations.

Through the fitted TCP, $I(z)$ can be approximated by the interference in Poisson cluster networks. According to Eq. (34) in [9], we have

$$\mathcal{L}_{I_{\rm PCP}}(s) = \exp\left\{-\lambda_l \int_{\mathbb{R}^2} \left[1-\exp(-\bar{c}\nu(s,y,z))\right]{\rm d}y\right\} \times \int_{\mathbb{R}^2} \exp(-\bar{c}\nu(s,y,z))f(y){\rm d}y, \quad (29)$$

where

$$\nu(s,y) = \int_{\mathbb{R}^2} \frac{f(x)}{1+(s\ell(x-y-z))^{-1}}{\rm d}x, \quad (30)$$

and $f(x)$ is the probability density function of the node distribution around the parent point. For the TCP, we have

$$f(x) = \frac{1}{2\pi\sigma^2}\exp\left(-\frac{\|x\|^2}{2\sigma^2}\right). \quad (31)$$

Substituting (29) into (23), the success probability is approximated as $P(\theta) \approx \mathcal{L}_{I_{\rm PCP}}(\theta r_{\rm d}^{\alpha})$.

Fig. 5 illustrates the success probabilities with PPP and TCP approximations for different ξ and $\lambda_{\rm p}$. The results show that the EPP-based transmission success probability can be approximated by the TCP-based results extremely well while the results in the PPP case have obvious deviations. The reason lies in the higher-order statistics of the EPP, which govern the interaction between nodes and strongly affect the success probability of the information transmission. Therefore, compared with the PPP, the PCP is a more suitable model for capturing the actual topology of the energized nodes, due to the positive energy correlation.

V. Conclusions

Since the locations of the RF-power sources are a common source of randomness, the harvested energy is correlated at nearby RF-powered node locations. This paper focused on the properties of the point process of nodes that successfully harvest enough energy from a Poisson field of RF transmitters, which is the first attempt to capture the energy correlation in wirelessly powered networks within a stochastic geometry-based framework. We derived the first- and second-order statistics for SEHM- and PEHM-based EPPs, respectively. The results indicate that the energized nodes exhibit clustering behavior, which is intuitive since if a node succeeds in harvesting enough energy, the nodes nearby are likely to succeed also, and vice versa. Furthermore, we used a fitted PCP to approximate the EPP, and the corresponding approximation of the transmission success probability coincides quite exactly with the simulation curve. Overall, both the analysis and approximation show that "attraction" exists between the energized node locations, and the widely used PPP-based model as well as the results derived from it deviate significantly from the exact ones.

Acknowledgment

The work of N. Deng has been supported by National Natural Science Foundation of China (61701071), the China Postdoctoral Science Foundation (2017M621129), the open research fund of National Mobile Communications Research Laboratory, Southeast University (No. 2019D03), the Fundamental Research Funds for the Central Universities (DUT16RC(3)119), and the work of M. Haenggi has been supported by the U.S. NSF (grant CCF 1525904).

References

[1] S. Bi, C. K. Ho, and R. Zhang, "Wireless powered communication: opportunities and challenges," *IEEE Communications Magazine*, vol. 53, no. 4, pp. 117–125, Apr. 2015.

[2] K. Huang and V. K. N. Lau, "Enabling wireless power transfer in cellular networks: Architecture, modeling and deployment," *IEEE Transactions on Wireless Communications*, vol. 13, no. 2, pp. 902–912, Feb. 2014.

[3] S. Akbar, Y. Deng, A. Nallanathan, M. Elkashlan, and A. Aghvami, "Simultaneous wireless information and power transfer in K-tier heterogeneous cellular networks," *IEEE Transactions on Wireless Communications*, vol. 15, no. 8, pp. 5804–5818, Aug 2016.

[4] Y. Liu, L. Wang, S. A. R. Zaidi, M. Elkashlan, and T. Q. Duong, "Secure D2D communication in large-scale cognitive cellular networks: A wireless power transfer model," *IEEE Transactions on Communications*, vol. 64, no. 1, pp. 329–342, Jan. 2016.

[5] L. Shi, L. Zhao, K. Liang, and H. Chen, "Wireless energy transfer enabled D2D in underlaying cellular networks," *IEEE Transactions on Vehicular Technology*, vol. 67, no. 2, pp. 1845–1849, Feb 2018.

[6] M. Haenggi, *Stochastic geometry for wireless networks*. Cambridge University Press, 2012.

[7] N. Deng and M. Haenggi, "The energy and rate meta distributions in wirelessly powered D2D networks," *IEEE Journal on Selected Areas in Communications*, 2018, available on IEEE Xplore Early Access.

[8] X. Lu, I. Flint, D. Niyato, N. Privault, and P. Wang, "Self-sustainable communications with RF energy harvesting: Ginibre point process modeling and analysis," *IEEE Journal on Selected Areas in Communications*, vol. 34, no. 5, pp. 1518–1535, May 2016.

[9] R. Ganti and M. Haenggi, "Interference and outage in clustered wireless ad hoc networks," *IEEE Transactions on Information Theory*, vol. 55, no. 9, pp. 4067–4086, 2009.